Online Analysis of H2S and SO2 via Advanced Mid-Infrared Gas Sensors

ARTICLE *in* ANALYTICAL CHEMISTRY · SEPTEMBER 2015

Impact Factor: 5.64 · DOI: 10.1021/acs.analchem.5b02730

4 AUTHORS:

João Flávio da Silveira Petruci
São Paulo State University
12 PUBLICATIONS **51** CITATIONS
SEE PROFILE

Andreas Wilk
Universität Ulm
15 PUBLICATIONS **98** CITATIONS
SEE PROFILE

Arnaldo Cardoso
São Paulo State University
87 PUBLICATIONS **769** CITATIONS
SEE PROFILE

Boris Mizaikoff
Universität Ulm
311 PUBLICATIONS **4,801** CITATIONS
SEE PROFILE

analytical chemistry

Article

pubs.acs.org/ac

Online Analysis of H_2S and SO_2 via Advanced Mid-Infrared Gas Sensors

João Flavio da Silveira Petruci,[†,‡] Andreas Wilk,[‡] Arnaldo Alves Cardoso,[†] and Boris Mizaikoff*[,‡]

[†]São Paulo State University, Department of Analytical Chemistry, UNESP, CEP 14800-970, Araraquara, São Paulo Brazil

[‡]University of Ulm, Institute of Analytical and Bioanalytical Chemistry, 89081, Ulm, Germany

Supporting Information

ABSTRACT: Volatile sulfur compounds (VSCs) are among the most prevalent emitted pollutants in urban and rural atmospheres. Mainly because of the versatility of sulfur regarding its oxidation state (2− to 6+), VSCs are present in a wide variety of redox-environments, concentration levels, and molar ratios. Among the VSCs, hydrogen sulfide and sulfur dioxide are considered most relevant and have simultaneously been detected within naturally and anthropogenically caused emission events (e.g., volcano emissions, food production and industries, coal pyrolysis, and various biological activities). Next to their presence as pollutants, changes within their molar ratio may also indicate natural anomalies. Prior to analysis, H_2S- and SO_2-containing samples are usually preconcentrated via solid sorbents and are then detected by gas chromatographic techniques. However, such analytical strategies may be of limited selectivity, and the dimensions and operation modalities of the involved instruments prevent routine field usage. In this contribution, we therefore describe an innovative portable mid-infrared chemical sensor for simultaneously determining and quantifying gaseous H_2S and SO_2 via coupling a substrate-integrated hollow waveguides (iHWG) serving as a highly miniaturized mid-infrared photon conduit and gas cell with a custom-made preconcentration tube and an in-line UV-converter device. Both species were collected onto a solid sorbent within the preconcentrator and then released by thermal desorption into the UV-device. Hydrogen sulfide is detected by UV-assisted quantitative conversion of the rather weak IR-absorber H_2S into SO_2, which provides a significantly more pronounced and distinctively detectable rovibrational signature. Modulation of the UV-device system (i.e., UV-lamp on/off) enables discriminating between SO_2 generated from H_2S conversion and abundant SO_2 signals. After optimization of the operational parameters, calibrations in the range of 0.75−10 ppmv with a limit of detection (LOD) at 77 ppbv for SO_2 and 207 ppbv for H_2S were established after 20 min of sampling time at 200 mL min^{-1}. Taking advantage of the device flexibility in terms of sampling time, flow-rate, and iHWG design facilitates tailoring the developed Preconcentrator-UV-device-iHWG device toward a wide variety of application scenarios ranging from environmental/atmospheric monitoring to industrial process monitoring and clinical diagnostics.

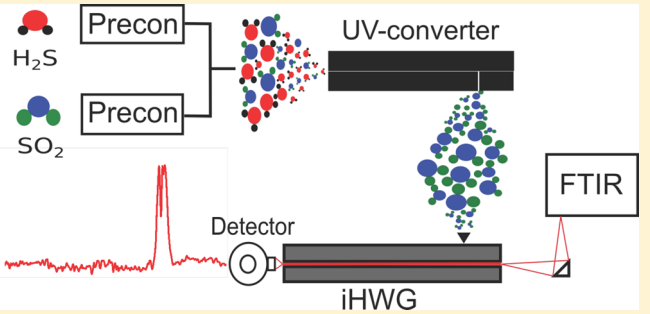

Hydrogen sulfide is a toxic, corrosive, and extremely malodorous gas.[1] Natural emissions of H_2S into the atmosphere predominantly relate to anaerobic bacteria reduction, degradation of organic matter, and volcanic activities.[2] Anthropogenic sources such as petroleum extraction, kraft paper mills, and fossil burning contribute a substantial amount of hydrogen sulfide emitted into the environment.[3]

According to the sulfur cycle,[4] once in the atmosphere H_2S is usually converted to higher-oxidative state sulfur constituents such as SO_2. Thereby, removal of gaseous sulfur via the water solubility of sulfate is facilitated.[5] Although it is a natural procedure, any disturbance of the equilibrium between these gaseous sulfur compounds may indicate localized air pollution events.[6] Besides, sulfur dioxide itself is also considered toxic and harmful and has been related to the increase of acid rain episodes in the 1980s.[7]

As a typical example, volcanic emissions contain several gases during and between eruptions.[8] The H_2S/SO_2 ratio depends on the occurrence of magmatic conditions and hydrothermal processes, thus providing an important indicator for forecasting and preventing volcanic eruption episodes.[9] Moreover, monitoring of H_2S and SO_2 in CO_2 streams is considered a quality and safety parameter during foodstuff production.[10] At a global scale, reliable data on H_2S and SO_2 emissions assists an increasing scientific understanding on the sulfur cycle and aids in modeling pollution distribution.

Hydrogen sulfide and sulfur dioxide are found in the environment at concentration levels ranging from low ppb to ppm.[11,12] At nonpolluted conditions, the detection limits for

Received: July 21, 2015
Accepted: September 14, 2015

DOI: 10.1021/acs.analchem.5b02730
Anal. Chem. XXXX, XXX, XXX−XXX

such trace gases are typically on the order of few ppbv. During volcanic eruptions, up to 6000 times more H_2S and up to 30 000 times more SO_2 has been detected compared to the tropospheric background.[13] Within the CO_2 added to mineral water, soda, and beers in the beverage industry, the concentration of H_2S and SO_2 must not exceed 0.5 and 2 ppmv, respectively.[10] In such application scenarios, a reliable analytical method that enables the simultaneous quantitative determination of hydrogen sulfide and sulfur dioxide within the same sample matrix is an essential demand.

Because of the low concentration of such sulfur gases, preconcentration techniques are usually required for enriching the sample prior to the analysis. Adsorption at solid state sorbent materials is among the most efficient and solvent-free methods for collecting volatile constituents.[14] Within the sorbent materials, usage of porous polymers is most common due to the ease of use, large breakthrough volumes, and facile desorption properties.[15] Previous studies have shown that Molecular Sieve 5A provided adequate trapping of gaseous sulfur compounds at ambient temperature with useful reproducibility.[16−20] After thermal desorption, sulfur constituents are usually quantified via laboratory analytical techniques. Gas chromatography is frequently applied and considered the "gold standard" for sulfur compound quantification with excellent sensitivity and precision.[17] However, the rather bulky dimensions and cost of instrumentation renders monitoring via GC techniques less feasible considering in-field scenarios or potential usage via drone- or unmanned aerial vehicle (UAV)-mounted sensing systems. Moreover, the direct use of sulfur-specific detectors does not allow for the discrimination between H_2S and SO_2, which in turn requires a prior separation step.

In the field of optical sensors, the mid-infrared (MIR; 3−20 μm) spectral range provides highly discriminatory molecular information due to the excitation of inherently specific fundamental vibrational and rovibrational transitions.[21] The detection of H_2S and SO_2 using infrared techniques has previously been described in the literature.[22−25] For example, Oppenheimer et al.[13] have highlighted the use of Fourier transform infrared (FT-IR) spectroscopy to analyze several volcanic gases including H_2S and SO_2. Ciaffoni et al.[24] demonstrated the potential of laser spectroscopy for determining VSCs. While some of these studies have achieved the required sensitivity, most of them rely on high-power lasers and extended-path gas cells owing to the rather weak absorption signature of H_2S in the MIR regime. The high instrumentation cost and bulky system dimensions to date limit extended field-applications of such MIR analyzer/sensor systems.

Our research team has recently demonstrated an innovative strategy improving in-field online monitoring of hydrogen sulfide using a new generation of highly miniaturized MIR waveguides.[26] Here, the detection is based on the in-flow UV-assisted conversion of H_2S to SO_2, which affords significantly stronger yet discriminatory absorption signatures within the 1400−1300 cm^{-1} spectral band. This sensor system comprises a UV-lamp, a compact and portable FTIR spectrometer, and a new generation of MIR waveguides simultaneously serving as a gas cell, i.e., so-called substrate-integrated hollow waveguides (iHWGs). Thereby, close to real-time determination of H_2S in a range of concentrations suitable for workplace safety monitoring (10−100 ppm) has been demonstrated.

Hollow waveguides are essentially considered highly miniaturized light-pipes with a coaxial hollow core usually made from dielectric materials that facilitate radiation propagation by reflection at the inside wall.[27] If gaseous samples are injected into the hollow core, the hollow waveguide (HWG) may simultaneously act as an extremely low volume gas cell with a well-defined optical absorption path length facilitating miniaturized MIR gas sensing strategies. The utility and adaptability of HWGs coupled to FT-IR spectrometers operating in the MIR spectral range for various gas sensing applications has extensively been described in the literature.[28−30]

Substrate-integrated hollow waveguide (iHWGs) constitute a new generation of hollow waveguides pioneered by the research team of Mizaikoff and collaborators[31] with exceptionally compact substrate dimensions (e.g., made from aluminum), an adaptable (i.e., designable) optical path length via integration of meandered hollow waveguide structures at virtually any desired geometry into an otherwise planar substrate, a minute volume of gas sample required for analysis (i.e., few hundreds of microliters), and the short transient residence time of these sample volumes within the active transducer region, thereby facilitating real-time monitoring and rendering iHWGs tailorable for a wide range of application scenarios.[26,32,33]

By combining a preconcentation device and a UV conversion system with the iHWG MIR sensor, we now demonstrate the simultaneous determination of H_2S and SO_2 in gaseous samples for the first time. Both gases were collected onto a solid sorbent and then thermally desorbed at 270 °C. Then, SO_2 was directly determined via its MIR signature, whereas in a second step H_2S was quantitatively converted into SO_2 using UV-irradiation. Thereafter, the H_2S signal is obtained after subtraction of the abundant SO_2 signal providing accurate and reliable results on both species.

EXPERIMENTAL SECTION

Hydrogen sulfide, sulfur dioxide, synthetic air, and nitrogen were acquired from MTI Industriegase AG (Neu-Ulm, Germany). The sample preconcentration tubes were custom-made from glass tubes in a U-shape with an inner diameter of 3.5 mm. The effective packaging length containing Molecular Sieve 5A (Sigma-Aldrich, St. Louis, MO) was 40 mm. Thermal desorption was performed using a heating wire wrapped around the tube and connected to a voltage/current controller (Basetech, BT-305, Germany). The H_2S−SO_2 conversion was achieved by exposing H_2S/synthetic air mixtures to UV radiation at 185 nm (UV Technik, Germany) using a custom-made quartz tube flow device with the tubular conversion cell coiled around the UV lamp (i.e., length of coiled segment, 95 cm). A gas mixing prototype based on mass flow controllers developed by the Institute of Analytical and Bioanalytical Chemistry at the University of Ulm and Lawrence Livermore National Laboratory (LLNL, Livermore, CA) was used for preparing and delivering gaseous sulfur species at varying concentrations dispersed in nitrogen at the desired flow rate (i.e., up to 200 mL min^{-1}).

All measurements were performed using a compact FT-IR spectrometer (Alpha OEM, Bruker Optics Inc., Ettlingen, Germany) equipped with a liquid nitrogen cooled mercury−cadmium-telluride (MCT) detector (FTIR-22.1.00, Infrared Associates, Stuart, FL). A straight-line iHWG made from polished aluminum providing an integrated hollow waveguide channel (i.e., absorption path length) of 15 cm at device dimensions of 150 mm × 46 mm × 17 mm (length × width ×

DOI: 10.1021/acs.analchem.5b02730
Anal. Chem. XXXX, XXX, XXX−XXX

depth) was coupled to the spectrometer using gold-coated off-axis parabolic mirrors with a focal length of 1 in. (Thorlabs, Dachau, Germany). The IR spectra were recorded in the wavelength range of 4000−650 cm^{-1} and at a spectral resolution of 4 cm^{-1}; 10 spectra were averaged per measurement unless stated otherwise. The OPUS 7.2 software package (Bruker Optics Inc., Ettlingen, Germany) was used for data acquisition.

The experimental setup is schematically shown in Figure 1. Polytetrafluoroethylene tubes with Luer-lock adapters were

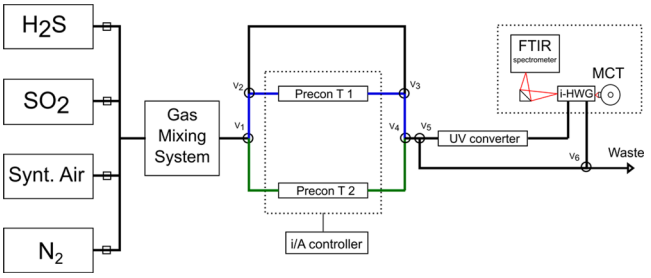

Figure 1. Scheme of the SO_2 and H_2S sample generation system coupled to the IR-iHWG sensor, a sample preconcentration steps and a custom H_2S-SO_2 conversion system using a coiled quartz tube (length of coiled segment: 95 cm), and an UV lamp emitting at 185 nm.

used to connect the system components. Three-way gas valves were adjusted for switching different sample pathways during a measurement routine. The calibration protocol was performed in five steps (a−e) as follows.

Standard Gas Mixtures. In order to prepare different concentrations of standard gas mixtures, suitable gas flow rates of H_2S, SO_2, and nitrogen were mixed and delivered to the sensing system at final flow rate of 200 mL min^{-1}. To obtain homogeneous solutions, the sample preparation was carried out for a period of 3 min. Hence, valves V_1, V_2, V_3, and V_4 were set to prevent the passage of the sample through the preconcentration tubes.

Sampling. By appropriately switching valves V_1, V_2, V_3, and V_4 samples were introduced into the preconcentration tubes at a gas flow rate of 200 mL min^{-1} for 20 min (i.e., resulting in 4 L of each sample). For the standard gas mixtures, the flow was regulated using the gas mixing system. For real-world samples, gas sampling bags containing air samples were attached to the preconcentration tubes, and the gas sample was transported through the system by suction using a pocket pump (model 222-3, SKC, Dorset, United Kingdom) with a calibrated gas flow of 200 mL min^{-1}.

Cleaning. After sampling, the valves V_1, V_2, and V_3 were set to close the preconcentration pathway. Nitrogen at 200 mL min^{-1} was used to rinse the system for 3 min. Thereafter, a background IR spectrum was collected averaging 100 scans.

Thermal Desorption/Data Acquisition. Next, the preconcentration tubes were heated (i.e., via the resistive heating wire controlled by a temperature-calibrated voltage/current controller at 5.3 A and 18.5 V). The optimized heating times were determined at 1 and 3 min for SO_2 and H_2S, respectively. For each analyte, the elution and detection procedure was performed as follows. (d_1) SO_2 determination: Nitrogen was inserted into preconcentration tube 1 via V_1, V_2, and V_3 at 20 mL min^{-1}. Thermally desorbed gases were then introduced in the iHWG via V_4 and V_5. The UV-converter was switched off. (d_2) H_2S determination: Synthetic air was inserted into preconcentrator tube 2 via V_1 and V_4 at 20 mL min^{-1}. Then, the desorbed gases were passed through the UV-converter via V_4 and V_5. The UV-lamp was switched on enabling conversion of H_2S to SO_2. The associated pushing flow, valves handling, and data acquisition were performed simultaneously during both experiments.

Data Evaluation. The peak area at 1395−1321 cm^{-1}, which is related to the V_3 vibro-rotational band of SO_2 was used for quantification of the obtained IR signals. The peak areas obtained during the d_1 experiments were directly related to the concentration of SO_2. By subtracting thus calculated peak areas from the signals obtained during the d_2 experiments, the signal associated with H_2S concentration was derived.

RESULTS AND DISCUSSION

Signal Optimization: SO_2. Several parameters were evaluated for maximizing the analytical signal within gaseous samples using preconcentration-based methods. After trapping, the SO_2 molecules were thermally desorbed into nitrogen with the desorption flow propagating the molecules into the detection component of the sensing system. Figure 2 shows

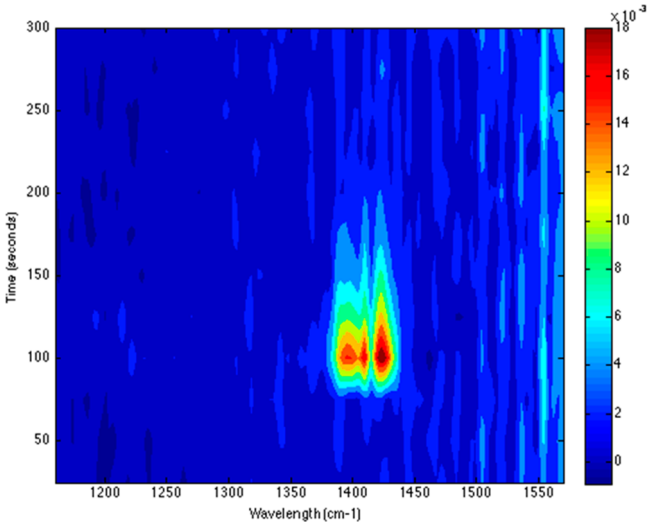

Figure 2. Contour plot (top view) of the SO_2 elution step. The absorption might be related to the color scale (blue, low and red, high).

the relation between the evaluated absorption signal within the 1600−1100 cm^{-1} band and time during the desorption procedure. At the beginning, no signal is evident, which is attributed to the dead volume between the iHWG and the preconcentration column. Approximately 90 s after sample desorption, the signal abruptly increased reaching a maximum value at approximately 100 s, which was then continuously decreasing again to zero (at approximately 200 s) until the entire desorbed plume has passed the iHWG. Similar to chromatography, narrow sample zones are preferable, as (i) a higher absorption signal amplitude is obtained providing for an improved signal-to-noise ratio (SNR) and (ii) for accelerating the cleaning and regeneration process (i.e., minimizing the time in between measurements in a quasi-continuous mode of operation). The desorption flow was optimized in the range from 5 to 30 mL min^{-1} at a SO_2 concentration of 10 ppm and is shown in Figure S-1 (Supporting Information). For all

DOI: 10.1021/acs.analchem.5b02730
Anal. Chem. XXXX, XXX, XXX−XXX

further experiments, a gas flow of 20 mL min^{-1} was subsequently used. The desorption temperature and time were also optimized, as illustrated in Figure S-2. Heating up to 270 °C for 1 min was determined as optimized desorption conditions for obtaining reliable SO_2 IR signals.

Signal Optimization: H_2S. Similarly to the SO_2 determination, H_2S molecules were thermally desorbed from the sorbent and carried into the detection system using an optimized gas flow rate. In order to circumvent the low absorptivity of H_2S in direct detection mode, the preconcentration and additional UV-based conversion step (into SO_2) was performed following:[26]

$$H_2S + HO^{\bullet} \rightarrow HS^{\bullet} + H_2O \quad (1)$$

$$HS^{\bullet} + O_2 \rightarrow SO + HO^{\bullet} \quad (2)$$

$$SO + 1/2O_2 \rightarrow SO_2 \quad (3)$$

In this scenario, apart from propagating the analyte molecules into the active transducer, the desorption flow is a crucial parameter for adapting the UV irradiation time at 185 nm such that quantitative conversion conditions are achieved. Hence, a variety of gas flow rates were evaluated at a concentration of 10 ppm of H_2S using synthetic air as the desorption matrix. As shown in Figure S-3, the optimum desorption flow rate was determined at 20 mL min^{-1}, while the desorption time provided an optimum value at 3 min (Figure S-4) at a desorption temperature of 270 °C for H_2S.

Sample Flow Rate. A chemical sensor combined with a gas phase preconcentration step may also be characterized by its efficiency in trapping molecules passing through the sorbent material. Usually, the trapping efficiency increases with the sample flow up to a maximum value and decreases afterward.[12,34] For the current configuration, a useful sample flow rate was evaluated ranging from 50 to 200 mL min^{-1}. The obtained results reveal an increasing analytical response with increasing sample flow rate in the given flow range. Sampling for 20 min was finally selected as a suitable period of time here; however, it could be adapted to other measurement scenarios and sampling requirements. Table 1 summarizes the obtained optimized conditions for quantitative SO_2 and H_2S studies with the developed IR sensing system.

Table 1. Summary of Optimized Parameters for Air Samples Preconcentration and Elution of SO_2 and H_2S

	value	
parameter	SO_2	H_2S
sampling time (min)	20	20
sampling flow (mL min^{-1})	200	200
desorption temperature (°C)	270	270
desorption time (min)	1	3
desorption flow (mL min^{-1})	20	20
UV lamp	off	on

Discrimination between SO_2 and H_2S IR Signals. The accuracy in discriminating between the analytical response provided by SO_2 and H_2S is the key parameter of the present study. Hence, two sets of experiments were performed: (s_1) A mixture containing 10 ppmv SO_2 and H_2S each was compared against a sample containing only 10 ppmv of SO_2, and (s_2) a mixture containing 1 ppm of SO_2 and 10 ppmv of H_2S was compared to a sample containing 1 ppmv of SO_2; all samples were subject to the same optimized SO_2 determination conditions. Considering the neat 10 and 1 ppm of SO_2 samples as quasi reference, the recovery rates vs the mixture samples were calculated providing values of 94.48 ± 2.89% and 91.73 ± 3.77%, respectively. This indicates that the presence of H_2S apparently neither affects the adsorption and desorption procedure nor the detection step.

Next, the influence of SO_2 on the H_2S determination was evaluated. For this purpose, again two sets of experiments were performed: (s_3) A mixture containing 10 ppmv SO_2 and H_2S each was compared against a sample of 10 ppmv H_2S and 10 ppmv SO_2 each, and (s_4) a mixture of 10 ppmv of SO_2 and 1 ppmv of H_2S was compared vs 1 ppmv of H_2S and 10 ppmv of SO_2. Both sample sets were analyzed at the optimized hydrogen sulfide determination conditions. Theoretically, the signal obtained for a mixture of both sulfur gases should be the sum of the independently obtained H_2S and SO_2 signals. Using the SO_2 response, it is then possible to calculate the H_2S signal after conversion by simple subtraction (i.e., the SO_2 signal = the peak area related to SO_2 standard sample; the H_2S signal = the peak area related of the sulfur mixture (after conversion) minus the neat SO_2 signal). Figure 3 illustrates the designed experimental sets.

In order to evaluate the accuracy, the obtained H_2S areas were compared to the standard H_2S samples at 10 and 1 ppmv designated as reference, determining recovery values of 94.40 ± 2.13% and 102.57 ± 4.88%, respectively. Evidently, the analytical response calculated for H_2S is suitably accurate. The obtained results of this performance study are summarized in Table 2.

Analytical Figures-of-Merit. Calibration functions were established enabling quantitative data analysis based on the evaluation of the peak area with integration boundaries from 1395 to 1321 cm^{-1} vs the SO_2 and H_2S concentration. For each concentration, the mean value of three replicate measurements was calculated. The proposed method revealed excellent linearity over the concentration range 0.75−10 ppmv of SO_2 ($r^2 > 0.997$) and H_2S ($r^2 > 0.990$), which was selected for the present study. The calculated limits of detection (LOD) were considered three times the standard deviation of the blank signal and were determined at 77 ppbv and 207 ppbv for SO_2 and H_2S, respectively. The obtained results are summarized in Table 3.

Evaluation of Spiked Real-World Samples. As real-world contaminated samples were not available during this study, the proposed method was tested for VSCs spiked into real-world outdoor air matrixes. For this purpose, a Tedlar gas sampling bag was filled with atmospheric air collected outdoors and quantitatively spiked with H_2S and SO_2 obtaining a final concentration of 5 ppmv for both gases. Thus, obtained samples were then inserted into the preconcentration system by suction using a pocket pump set at 200 mL min^{-1} for 20 min and then treated as described for the calibration samples herein. The concentration of H_2S and SO_2 derived from the calibration functions were 4.82 ± 0.78 ppmv and 4.73 ± 0.90 ppmv, respectively. Despite the substantial additional preconcentration of CO_2 from ambient air samples, it was demonstrated that no interference in trapping efficiency of the sorbent for the sulfur gases was observed. Besides, the CO_2 absorption signature occurs in the spectral range of 2400−2300 cm^{-1}, which furthermore limits any spectral interference during IR data evaluation. Similarly, water vapor has a high affinity to the applied sorbent material and is unavoidably cotrapped.

DOI: 10.1021/acs.analchem.5b02730
Anal. Chem. XXXX, XXX, XXX−XXX

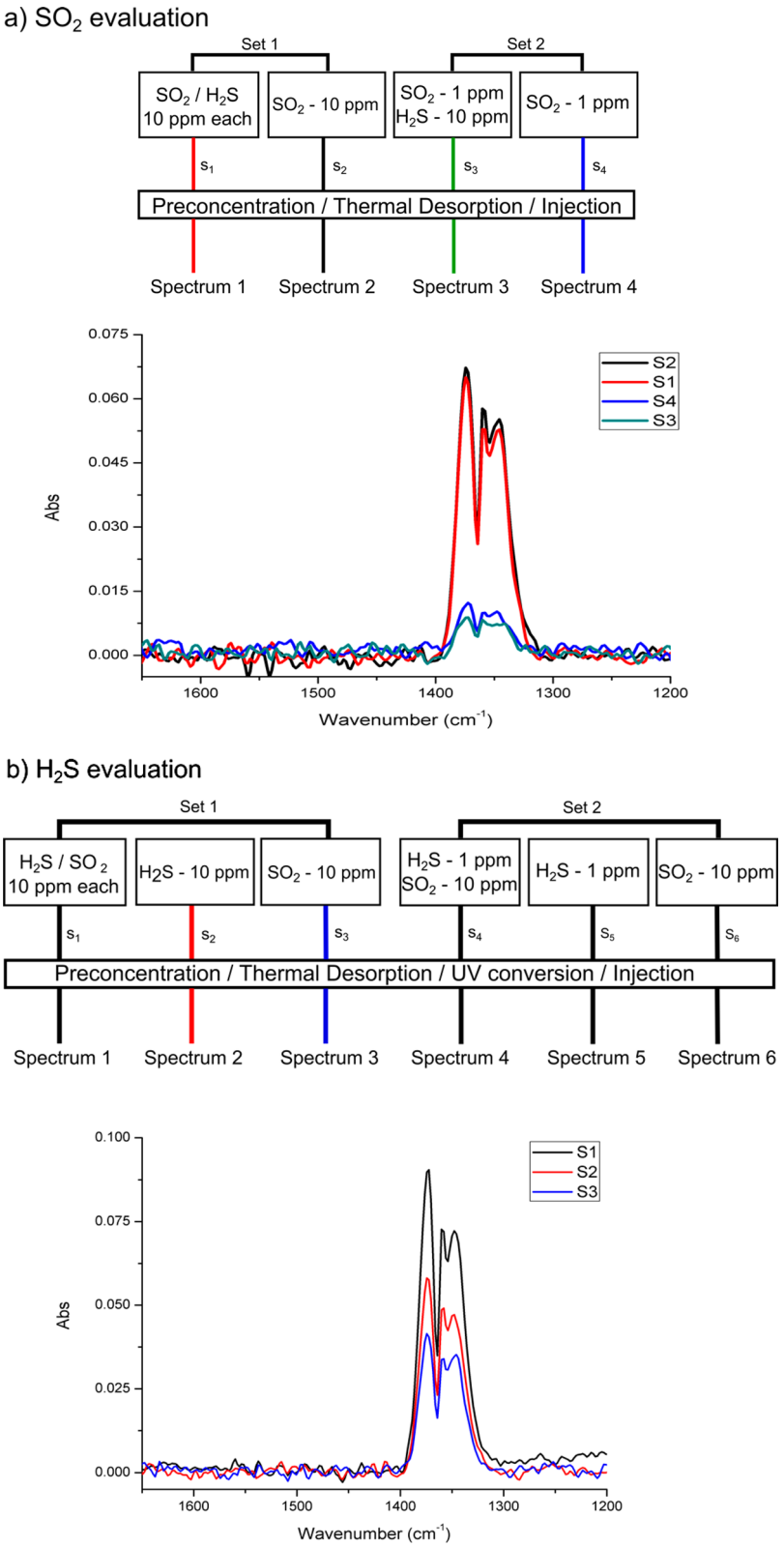

Figure 3. Experimental procedure for the quantification of and discrimination between (a) SO_2 and (b) H_2S.

However, since water molecules are strongly bound to the sorbent and are only released at the end of the desorption procedure, no spectral interference during collection of the IR signal of the sulfur species was noticed. Figure 4 shows exemplary IR spectra of the 5 ppmv H_2S and SO_2 samples in ambient air after preconcentration and desorption.

CONCLUSIONS

In this study, we described an innovative mid-infrared chemical sensor system for the simultaneous quantitative determination of gaseous H_2S and SO_2 by combining a new generation of substrate-integrated hollow waveguides (also known as iHWGs) with a miniaturized sample preconcentration and a

DOI: 10.1021/acs.analchem.5b02730
Anal. Chem. XXXX, XXX, XXX−XXX

Table 2. Summary of the Interference Experiments among H_2S and SO_2 Determination

analytical method	sample	SO_2 peak area	recovery (%)
SO_2 method	SO_2 + H_2S (10 ppm each)	3.257 ± 0.291	94.48 ± 2.89
	SO_2 + H_2S (1 and 10 ppm)	0.355 ± 0.084	91.73 ± 3.77
	SO_2 10 ppm	3.447 ± 0.112	
	SO_2 1 ppm	0.387 ± 0.058	
H_2S method	H_2S + SO_2 (10 ppm each)	3.666 ± 0.301	94.40 ± 2.13
	H_2S + SO_2 (1 and 10 ppm)	1.893 ± 0.128	102.57 ± 4.88
	H_2S 10 ppm	2.300 ± 0.133	
	H_2S 1 ppm	0.388 ± 0.076	
	SO_2 10 ppm	1.495 ± 0.066	

UV-converter system. While SO_2 is detected directly after thermal desorption, H_2S is instantaneously and quantitatively converted to SO_2 using UV-irradiation at 185 nm. This photolytically induced reaction is performed due to the rather weak IR absorption signature of H_2S. Given the rapid and efficient conversion procedure, the obtained SO_2 signal may be directly correlated to the initial H_2S concentration, and may be discriminated from abundant SO_2 by subtraction, thereby enabling the quantification of both molecules in mixture. The proposed methodology facilitates a limit of detection of 77 and 207 ppbv for SO_2 and H_2S, respectively, for a sampling time of 20 min at an overall sample flow rate of 200 mL min^{-1}. Consequently, the developed method is suitable for monitoring scenarios exceeding the atmospheric background concentration of sulfur gases and for moderate temporal resolution. However, the sensitivity of the method may be further improved by increasing the sampling flow rate and analysis time, and by increasing the absorption path length provided by the iHWG, as well as by using more efficient sorbent materials. Thereby, adapting the developed sensing strategy to a wide range of monitoring demands is enabled.[35]

In future, a significant reduction of the physical dimensions of the developed IR chemical sensing device is anticipated by replacing the FT-IR spectrometer with a suitable tunable quantum cascade laser (tQCL) light source. In addition, using an integrated and automated sample preconcentration device (iPRECON) along with a likewise compact UV-conversion system (iCONVERT), as described in the associated technical note facilitates the development of multifunctional and highly adaptable MIR gas sensing systems.[36,37]

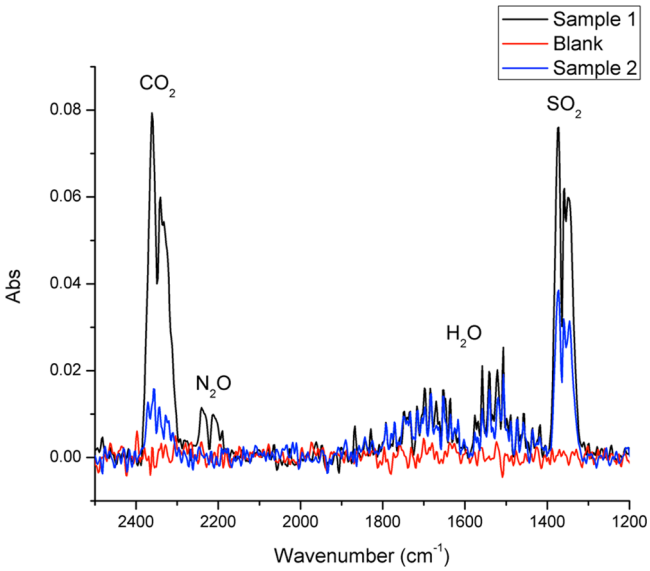

Figure 4. IR spectra obtained after sample preconcentration of air samples spiked with hydrogen sulfide and sulfur dioxide at a concentration of 5 ppm recorded using the IR-iHWG sensor at a spectral resolution of 4 cm^{-1}. The blue-line spectrum (sample 2) was obtained using optimized conditions for SO_2 determination, and the black-line spectrum (sample 1) was obtained using optimized conditions for H_2S determination.

■ ASSOCIATED CONTENT

Supporting Information

The Supporting Information is available free of charge on the ACS Publications website at DOI: 10.1021/acs.analchem.5b02730.

Evaluation of experimental conditions effects on sample preconcentration (PDF)

■ AUTHOR INFORMATION

Corresponding Author

*E-mail: boris.mizaikoff@uni-ulm.de.

Notes

The authors declare no competing financial interest.

■ ACKNOWLEDGMENTS

J.F.d.S.P. thanks FAPESP (Grant 2014/23974-3) for financial support during a research stay at IABC-UULM. B.M. acknowledges partial support of this study by the project APOSEMA funded by the German BMBF within the M-Era.net program. This work was performed in part under the auspices of the U.S. Department of Energy by Lawrence Livermore National Laboratory (LLNL) under Contract DE-AC52-

Table 3. Analytical-Figures-of-Merit Obtained for the IR-iHWG Hydrogen Sulfide and Sulfur Dioxide Gas Sensing Systems

	value	
parameter	H_2S	SO_2
limit of detection (3 × SD of blank)	0.207 ppm	0.077 ppm
limit of quantification (10 × SD of blank)	0.69 ppm	0.26 ppm
correlation coefficient	0.9907	0.9976
linear range	0.75−10 ppm	0.75−10 ppm
regression equation	$A = 0.295[H_2S] - 0.0011$	$A = 0.5876[SO_2] - 0.2204$

DOI: 10.1021/acs.analchem.5b02730
Anal. Chem. XXXX, XXX, XXX−XXX

07NA27344. This project was funded under LLNL Subcontract Nos. B598643 and B603018.

REFERENCES

(1) Guidotti, T. L. *Int. J. Toxicol.* **2010**, *29*, 569−581.
(2) Campos, V. P.; Oliveira, A. S.; Cruz, L. P. S.; Borges, J.; Tavares, T. M. *Microchem. J.* **2010**, *96*, 283−289.
(3) Susaya, J.; Kim, K.-H.; Phan, N. T.; Kim, J. C. *Atmos. Environ.* **2011**, *45*, 3381−3390.
(4) Berglen, T. F. *J. Geophys. Res.* **2004**, *109*, D19310.
(5) Davinson, B.; O'Dowd, C.; Hewitt, C. N.; Smith, M. H.; Harrison, R. M.; Peel, D. A.; Wolf, E.; Mulvaney, R.; Schwikowski, M.; Baltensperger, U. *Atmos. Environ.* **1996**, *30*, 1895−1906.
(6) De Souza, T. L.; Bhatia, S. P. *Anal. Chem.* **1976**, *48*, 2234−2240.
(7) Cheng, R. J.; Hwu, J. R.; Kim, J. T.; Leu, S. M. *Anal. Chem.* **1987**, *59*, 104A−106A.
(8) Andreae, M. O. *Mar. Chem.* **1990**, *30*, 1−29.
(9) O'Dwyer, M.; Padgett, M.; McGonigle, J. S.; Oppenheimer, C.; Inguaggiato, S. *Geophys. Res. Lett.* **2003**, *30*, 12−15.
(10) Stankova, M.; Vilanova, X.; Calderer, J.; Llobet, E.; Ivanov, P.; Gracia, I.; Cané, C.; Correig, X. *Sens. Actuators, B* **2004**, *102*, 219−225.
(11) Toda, K.; Dasgupta, P. K.; Li, J.; Tarver, G. A.; Zarus, G. M. *Anal. Chem.* **2001**, *73*, 5716−5724.
(12) Petruci, J. F. S.; Cardoso, A. A. *Anal. Methods* **2015**, *7*, 2687−2692.
(13) Oppenheimer, C.; Francis, P.; Burton, M.; Maciejewski, A. J. H.; Boardman, L. *Appl. Phys. B: Lasers Opt.* **1998**, *67*, 505−515.
(14) Wardencki, W. *J. Chromatogr. A* **1998**, *793*, 1−19.
(15) Black, M. S.; Herbst, R. P.; Hitchcock, D. R. *Anal. Chem.* **1978**, *50*, 848−851.
(16) Bollman, D. H.; Mortimore, D. M. *J. Chromatogr. Sci.* **1972**, *10*, 523−527.
(17) Pandey, S. K.; Kim, K. H. *Environ. Sci. Technol.* **2009**, *43*, 3020−3029.
(18) Shooter, D.; de Mora, S. J.; Grout, A.; Wylie, D. J.; Zhi-yun, H. *Int. J. Environ. Anal. Chem.* **1992**, *47*, 239−249.
(19) Davison, B. M.; Allen, A. G. *Atmos. Environ.* **1994**, *28*, 1721−1729.
(20) Tuan, H. P.; Janssen, H. G.; Cramers, C. A.; Smit, A. L. C.; Van Loo, E. M. *J. High Resolut. Chromatogr.* **1994**, *17*, 373−389.
(21) Mizaikoff, B. *Chem. Soc. Rev.* **2013**, *42*, 8683−8699.
(22) McCurdy, M. R.; Bakhirkin, Y.; Wysocki, G.; Lewicki, R.; Tittel, F. K. *J. Breath Res.* **2007**, *1*, 014001.
(23) Dong, F.; Junaedi, C.; Roychoudhury, S.; Gupta, M. *Anal. Chem.* **2011**, *83*, 4132−4136.
(24) Ciaffoni, L.; Peverall, R.; Ritchie, G. A. D. *J. Breath Res.* **2011**, *5*, 024002.
(25) Kim, J. B.; Kim, Y. G. *Int. Symp. Commun. Inf. Technol.* **2009**, 1489−1491.
(26) Petruci, J. F. S.; Fortes, P. R.; Kokoric, V.; Wilk, A.; Raimundo, I. M., Jr.; Cardoso, A. A.; Mizaikoff, B. *Analyst* **2014**, *139*, 198−203.
(27) Young, C. R.; Menegazzo, N.; Riley, A. E.; Brons, C. H.; DiSanzo, F. P.; Givens, J. L.; Disko, M. M.; Mizaikoff, B. *Anal. Chem.* **2011**, *83*, 6141−6147.
(28) Thompson, B. T.; Inberg, A.; Croitoru, N.; Mizaikoff, B. *Appl. Spectrosc.* **2006**, *60*, 266−271.
(29) Frey, C. M.; Luxenburger, F.; Droege, S.; Mackoviak, V.; Mizaikoff, B. *Appl. Spectrosc.* **2011**, *65*, 1269−1274.
(30) Young, C.; Cendejas, R.; Howard, S. S.; Sanchez-Vaynshteyn, W.; Hoffman, A. J.; Franz, K. J.; Yao, Y.; Mizaikoff, B.; Wang, X.; Fan, J.; Gmachl, C. F. *Appl. Phys. Lett.* **2009**, *94*, 091109.
(31) Wilk, A.; Carter, J. C.; Chrisp, M.; Manuel, A. M.; Mirkarimi, P.; Alameda, J. B.; Mizaikoff, B. *Anal. Chem.* **2013**, *85*, 11205−11210.
(32) Perez-Guaita, D.; Kokoric, V.; Wilk, A.; Garrigues, S.; Mizaikoff, B. *J. Breath Res.* **2014**, *8*, 026003.
(33) Petruci, J. F. S.; Fortes, P. F.; Kokoric, V.; Wilk, A.; Raimundo, I. M., Jr.; Cardoso, A. A.; Mizaikoff, B. *Sci. Rep.* **2013**, *3*, 03174.
(34) Felix, E. P.; Cardoso, A. A. *J. Braz. Chem. Soc.* **2012**, *23*, 142−147.
(35) Fortes, P. R.; Petruci, J. F. S.; Wilk, A.; Cardoso, A. A.; Raimundo, I. M., Jr.; Mizaikoff, B. *J. Opt.* **2014**, *16*, 094006.
(36) Kokoric, V.; Wilk, A.; Mizaikoff, B. *Anal. Methods* **2015**, *7*, 3664−3667.
(37) Petruci, J. F. S.; Cardoso, A. A.; Wilk, A.; Kokoric, V.; Mizaikoff, B. *Anal. Chem.* **2015**, DOI: 10.1021/acs.analchem.5b02731.

DOI: 10.1021/acs.analchem.5b02730
Anal. Chem. XXXX, XXX, XXX−XXX